ChemComm

Spectroscopic Observation and Structure-Insensitivity of Hydroxyls on Gold

Journal:	*ChemComm*
Manuscript ID	CC-COM-01-2022-000283.R1
Article Type:	Communication

COMMUNICATION

Spectroscopic Observation and Structure-Insensitivity of Hydroxyls on Gold

Received 00th January 20xx,
Accepted 00th January 20xx

DOI: 10.1039/x0xx00000x

Yiteng Zheng,[a] Yue Qi,[b] Ziyu Tang,[b] Junzhi Tan,[a] Bruce E. Koel,*[a] Simon G. Podkolzin*[b]

The O-H stretching vibration of surface hydroxyls remained at 3691 cm^{-1} for gold structures ranging in size from clusters to nanoparticles, to non-flat bulk surfaces. In contrast, this vibration was not observed on flat gold surfaces. Therefore, this vibration can serve as an indicator of the roughness of the gold surface and associated functional properties, such as catalytic activity.

Gold structures ranging in size from subnanometer clusters with just a few Au atoms, to nanometer particles to microscopic and macroscopic particles, to bulk surfaces are used in numerous and diverse science and technology applications. High catalytic activities and selectivities of Au structures, especially in hydrocarbon oxidation reactions, offer tremendous opportunities for developing environmentally-friendly and energy-efficient technologies. In all applications, except for completely dehydrated systems, hydroxyls are likely present on Au surfaces, and their presence may change catalytic and other properties. For example, hydroxyls on Au are important in the bio-inspired synthesis of nanocomposites,[1] solar energy conversion,[2] biomolecule interactions[3] and clinical tumor imaging and therapy.[4] In catalysis, hydroxyls were shown to play an important role in the water-gas shift reaction[5] as well as in CO and alcohol oxidation over Au catalysts.[6] Despite their importance, hydroxyls on Au have not been observed or characterized. In this work, a direct observation of hydroxyls on Au with in situ diffuse reflectance infrared Fourier transform spectroscopy (DRIFTS) is reported.

Moreover, oxygen and hydrocarbon structures on Au surfaces are highly dependent on the size of Au particles. While flat surfaces of bulk Au are practically chemically inert, coordinatively unsaturated surface Au atoms in nanoparticles and subnanometer clusters readily adsorb hydrocarbons, oxygen as well as other molecules and, thus, catalyze numerous reactions. As an example, our study with monodisperse 5, 50 and 400-nm Au particles showed that the rate of catalytic H_2O_2 decomposition increased dramatically with decreasing Au particle size when the total number of surface Au atoms was kept constant.[7, 8] For adsorbates, experimental and computational studies demonstrate that adsorption energies and, consequently, geometries and vibrational frequencies of atomic and molecular oxygen on Au surfaces are highly dependent on the size of Au particles.[7-9] As an example, while molecular oxygen on Au(111) is unstable, its adsorption becomes progressively more energetically favorable with decreasing Au particle size. The O-O bond distance gradually increases, and its stretching vibration, ν(O-O), accordingly, progressively decreases from 1185 cm^{-1} for a bulk Au surface to 1049 cm^{-1} for a subnanometer-size Au cluster.[7, 8] Similarly for atomic oxygen, as an O atom becomes more strongly bound to smaller Au particles, its O-Au distances progressively decrease and, accordingly, ν(O-Au) increases from 373 to 467 cm^{-1}.[7, 8] As another example, for dissociative H_2 adsorption, the Au-H bond becomes progressively stronger with decreasing Au particle size.[9] In this work, DRIFTS experimental measurements with Au particles of different sizes and density functional theory (DFT) calculations for Au surfaces ranging from subnanometer clusters to bulk Au show that in contrast with oxygen and other adsorbate structures that are highly sensitive to the Au particle size, hydroxyls are structure insensitive.

Au was deposited on a ZSM-5 (Si/Al=15) support using the incipient wetness impregnation method, which ensures that all deposited metal is on the support. Our previous catalytic studies with supported Au and other metals successfully used the same preparation method.[9-15] The Au loading was varied between 0.25 and 2 wt %. Details of the experimental and computational methods are provided in the Supplementary Information. Hydroxyls on the ZSM-5 zeolite support are structure sensitive: their vibrational frequencies depend on the adsorption site. The two prominent peaks at 3737 and 3598 cm^{-1} in the in situ DRIFTS spectra in Figure 1a, collected in a flow of dry synthetic air at 373 K, are due to the O-H bond stretching vibrations, ν(O-H), of hydroxyls on Si and Al sites of the ZSM-5 framework, respectively.[12-14] The two additional peaks at 3650 and 3779 cm^{-1} are due to hydroxyls on extraframework (EF) Al sites.[12-14] The new DRIFTS peak at 3691 cm^{-1} observed after the

[a] Department of Chemical and Biological Engineering, Princeton University, Princeton, New Jersey 08544, United States.
[b] Department of Chemical Engineering and Materials Science, Stevens Institute of Technology, Hoboken, New Jersey 07030, United States.

Electronic Supplementary Information (ESI) available: Details of the experimental and computational methods are provided. See DOI: 10.1039/x0xx00000x

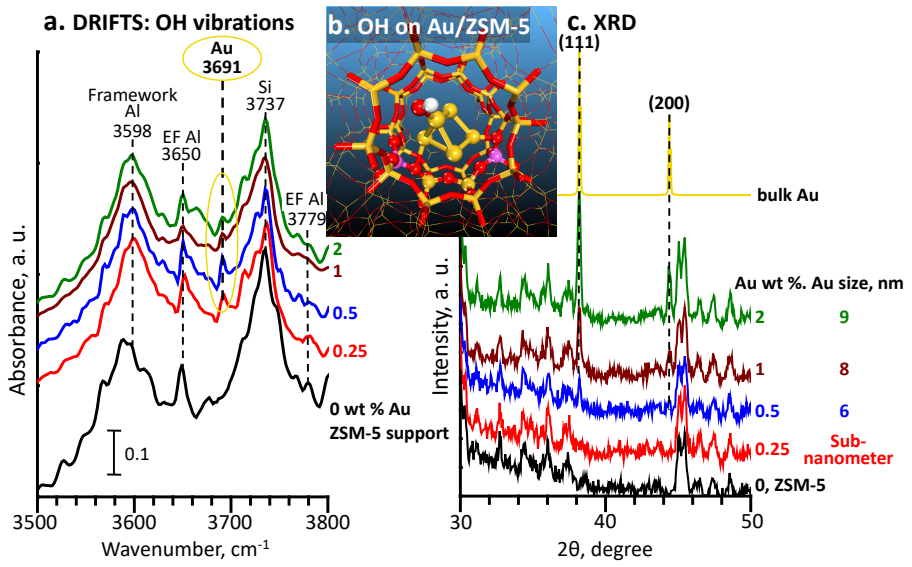

Figure 1. (**a**) DRIFTS spectra for ZSM-5 without Au and 0.25-2 wt % Au/ZSM-5 in a flow of dry synthetic air at 373 K after dehydration at 573 K, (**b**) DFT model of OH on a Au_5 cluster anchored inside a ZSM-5 pore and (**c**) XRD patterns for ZSM-5 without Au and 0.25-2 wt % Au/ZSM-5.

Au deposition in Figure 1a must be due to ν(O-H) of hydroxyls on Au. The calculated ν(O-H) of 3695 cm^{-1} for a hydroxyl on a Au_5 particle anchored inside a zeolite pore in Figure 1b confirms this assignment. The Au_5 particle in the model is bonded to a double framework Al-atom site, which was found to be preferential in our experimental and computational studies for anchoring of Mo and Cr in zeolites.[10, 12-14]

The presence of water on Au can be ruled out because the catalysts were dehydrated in a flow of dry synthetic air at 573 K for 1 h prior to the spectra collection at 373 K in the same air flow. In addition, the characteristic vibrations for water adsorbed on Au are not observed in our spectra: the water deformation, δ(HOH), at 1616-1654 cm^{-1} and ν(O-H) of water at ~3500 cm^{-1}.[16, 17]

The X-ray diffraction (XRD) measurements in Figure 1c demonstrate that the size of Au nanoparticles increased as the concentration of Au increased from 0.25 to 2 wt %. At the lowest Au concentration of 0.25 wt %, the XRD peaks at 38.1° for Au(111) and 44.3° for Au(200) are not well resolved, indicating that Au was mostly present in the form of subnanometer clusters. The diameter of the largest pore in the ZSM-5 zeolite is 0.55 nm with the size of intersection cavities of 0.9 nm, which puts a restriction on the size of Au particles located in the pores. A representative TEM image in Figure 3c confirms that most metal particles for 0.25 wt % Au/ZSM-5 had the size of less than 1 nm with a small number of isolated 1-2-nm particles. For higher Au concentrations, the Au particles located in the pores had the same size of less than 1 nm. However, additional particles located on the outer surface of the zeolite became progressively larger with increasing Au loading. The line broadening of the XRD Au peaks in Figure 1c and an analysis of TEM images show that the average Au particle size increased to 6, 8 and 9 nm for 0.5, 1 and 2 wt % Au, respectively.

The position of the DRIFTS peak for OH on Au in Figure 1a remains at 3691 cm^{-1} for all Au concentrations, even though the Au particles size increases from subnanometer to 9 nm. The DFT results in Figure 2 demonstrate that this experimentally observed structure insensitivity of hydroxyls on Au in a limited range of Au particle sizes is actually valid for a wide range of Au surfaces: from Au_3 to Au_{13} clusters, to a Au_{55} particle with a size of ~1 nm, to stepped surfaces of bulk Au: Au(511), Au(211) and Au(111) with an adatom. Similar cluster and periodic structure models were previously successfully used to describe oxygen, H_2O_2 and OOH adsorption on Au and other adsorbates on multiple surfaces.[9, 13, 15, 18-28] The calculations show that on most Au surfaces hydroxyls preferentially adsorb on a bridge Au-Au site, with ν(O-H) being in a narrow range from 3683 to 3687 cm^{-1} (Figure 2). Slightly higher wavenumbers, 3689-3705 cm^{-1}, are calculated for hydroxyls on an atop site bonding to a single Au atom when it is an adatom, on the Au_3 cluster (Figure 2) or when a small Au cluster is anchored on a zeolite (Figure 1b). Additional calculations for the Au_{55} particle and periodic surfaces show that the ν(O-H) wavenumbers change within ±15 cm^{-1}, depending on the position and orientation of the hydroxyls. Therefore, since the ν(O-H) values for both the atop- and bridge-bonded hydroxyls are close, it is likely that they are observed as a single peak at 3691 cm^{-1} in the experimental spectra in Figure 1a.

The calculated results for additional OH vibrations in Table S1 provide guidance on distinguishing atop- and bridge-bonded OH groups. The corresponding Au-O and O-H bond distances are provided in Table S2. While there is only one stretching vibration of the Au-O bond, ν(Au-OH), for atop-bonded OH calculated to be at 493-525 cm^{-1}, there are two stretching vibrations at lower wavenumbers for bridge-bonded OH: symmetric, ν_s(Au-OH), at 311-376 cm^{-1} and asymmetric, ν_a(Au-OH), at 233-340 cm^{-1}. Similarly for the OH bending mode, there is a single vibration, δ(Au-OH), at 820-846 cm^{-1} for atop-bonded OH, and two δ(Au-OH) vibrations at lower wavenumbers for bridge-bonded OH at 556-705 cm^{-1} for the mostly vertical movement of the H atom and 735-807 cm^{-1} for the mostly horizontal movement of the H atom. All these additionally calculated vibrations are lower than the transparency limit of the ZnSe windows of the in situ cell used in our DRIFTS measurements and, therefore, they were not observed experimentally.

Flat Au surfaces represent a special case. Although Au(111) and other flat surfaces became increasingly dominant for the larger and more crystalline Au nanoparticles in 0.5-2 wt % Au/ZSM-5 materials, the calculated ν(O-H) for hydroxyls on Au(111) at a lower wavenumber of 3668 cm^{-1} (Figure 2) was not observed experimentally in the DRIFTS spectra (Figure 1a). Additional

calculations for Au(111) show that the ν(O-H) wavenumbers can be even lower at 3648 cm^{-1}, depending on the position and orientation of the hydroxyls on the preferential bridge site. Moreover, the intensity of the DRIFTS peak at 3691 cm^{-1} for OH on non-flat Au surfaces remained mostly constant with increasing Au particle size. Therefore, hydroxyls were not present on Au(111) under the experimental conditions in a flow of dry synthetic air at 373 K after dehydration at 573 K. A contributing factor can be a lower infrared intensity of ν(O-H) on larger Au particles due to the metal-surface selection rule,[29] making a small number of hydroxyls on flat surfaces of larger particles after dehydration not detectable spectroscopically. As the Au particle size increased, a larger number of surface Au atoms were located on Au(111) and other flat surfaces and, thus, the number of hydroxyls on non-flat Au sites with ν(O-H) at 3691 cm^{-1} did not significantly change with increasing Au loading.

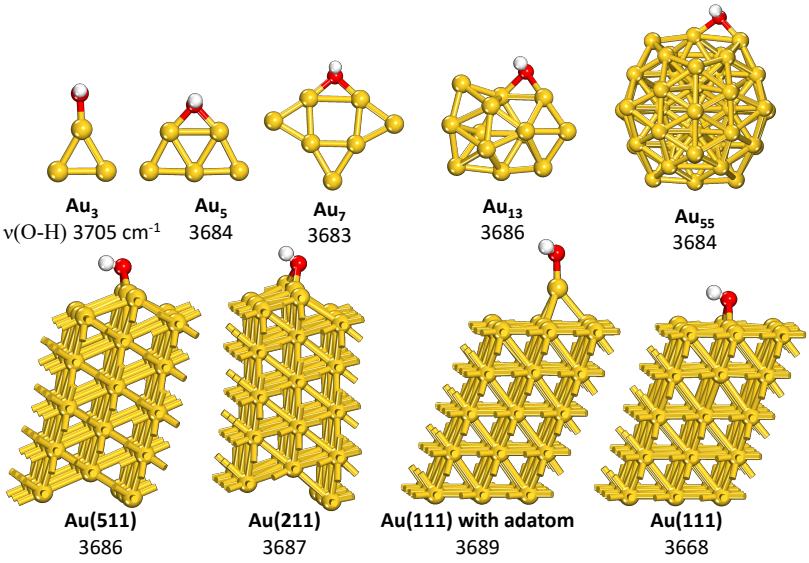

Figure 2. Geometries of hydroxyls on Au surfaces ranging from Au_3-Au_{13} clusters, to a Au_{55} particle with a size of ~1 nm and to periodic bulk Au surfaces obtained with DFT calculations. The listed numbers are calculated O-H bond stretching vibrational frequencies, ν(O-H), cm^{-1}.

If hydroxyls are indeed not present on flat Au surfaces, which are known to be mostly chemically inert and, in contrast, hydroxyls are present and structure-insensitive on coordinatively unsaturated surface Au atoms of Au clusters, small Au nanoparticles and other non-flat Au surfaces, the presence of the stretching vibration for OH on Au at 3691 cm^{-1} after dehydration can serve as a useful simple indicator of catalytic activity and other functional properties that depend on the roughness of Au surfaces. To test this hypothesis, the catalytic activity of 0.25 wt % Au/ZSM-5 was evaluated in selective ethanol oxidation with gas-phase oxygen in a flow reactor system previously used for studying acetic acid hydrodeoxygenation.[30] Since this catalyst had mostly subnanometer-size Au clusters, the Au dispersion was practically 100%. For comparison, 3.6 wt % Au was deposited on an amorphous SiO_2 support. The 3.6 wt % Au/SiO_2 catalyst had significantly larger Au particles with an average size of 15 nm based on TEM (Figures 3c and S2) and XRD (Figure S1) measurements, corresponding to 7% Au dispersion. However, the metal loading of the 3.6 wt % Au/SiO_2 catalyst was chosen such that both catalysts had the same number of surface Au atoms, 13 $\mu mol_{Au}/g_{catalyst}$.

While the vibration for OH on Au was observed at 3691 cm^{-1} for 0.25 wt % Au/ZSM-5, it was not observed for 3.6 wt % Au/SiO_2 (Figure 3a). Only a single peak at 3737 cm^{-1} for OH on Si sites was observed for 3.6 wt % Au/SiO_2 (Figure 3a). The absence of the peak at 3691 cm^{-1} indicates that most surface Au atoms were located on flat surfaces and that the number of Au atoms on non-flat surfaces was small, which is consistent with the large size of Au particles of 15 nm on SiO_2.

The 0.25 wt % Au/ZSM-5 catalyst was highly efficient in selective ethanol oxidation with gas-phase oxygen (Figure 3b). Whereas the blank ZSM-5 zeolite support was not catalytically active at 333 K, the 0.25 wt % Au/ZSM-5 catalyst exhibited a high initial reaction rate of 122 1/h in turnover frequency (TOF) units: ethanol molecules reacted per surface Au atom per hour. The initial rate declined and then stabilized at 116 1/h after 2.5 h of time on stream. The reaction products were ethyl acetate, acetaldehyde and acetic acid (Table S3). Undesirable overoxidation reactions to CO and CO_2 were completely avoided. In contrast, 3.6 wt % Au/SiO_2 was significantly less active with a stabilized activity of 12 1/h after 2.5 h. The reaction products remained the same, but with a larger concentration of acetic acid (Table S3). Blank SiO_2, like blank ZSM-5, was inert under the reaction conditions. In an additional experiment, when 3.6 wt % Au/SiO_2 and blank ZSM-5 were physically mixed at a weight ratio of 1:1 and tested for catalytic activity, the number of reacting ethanol molecules per Au surface atom remained the same. Therefore, the presence of Al sites in the zeolite by itself did not affect the reaction rate, and the lower activity of 3.6 wt % Au/SiO_2 was due exclusively to the larger size of its Au particles. Accordingly, the presence of ν(O-H) at 3691 cm^{-1} for 0.25 wt % Au/ZSM-5 indicates the presence of coordinatively unsaturated Au surface sites, which have high catalytic activity, and the absence of ν(O-H) for 3.6 wt % Au/SiO_2 indicates a lack of such Au active sites. These results confirm that the presence of the O-H stretching vibration for hydroxyls on Au is, indeed, a qualitative indicator of the roughness of Au surfaces and, thus, functional properties that depend on it, such as catalytic activity.

In summary, the O-H stretching vibration of hydroxyls on Au surfaces was observed with in situ DRIFTS measurements. This vibration remained at 3691 cm^{-1} when the size of supported Au particles increased from subnanometer to 9 nm. The size of Au particles was determined with XRD and TEM measurements. DFT calculations show that this structure-insensitivity of hydroxyls on Au is valid for a wide range of Au structures: from clusters with just a few atoms to nanoparticles, to non-flat surfaces of bulk Au. In contrast, this vibration was not observed on flat Au surfaces. Therefore, this vibration can serve as a qualitative indicator of the roughness

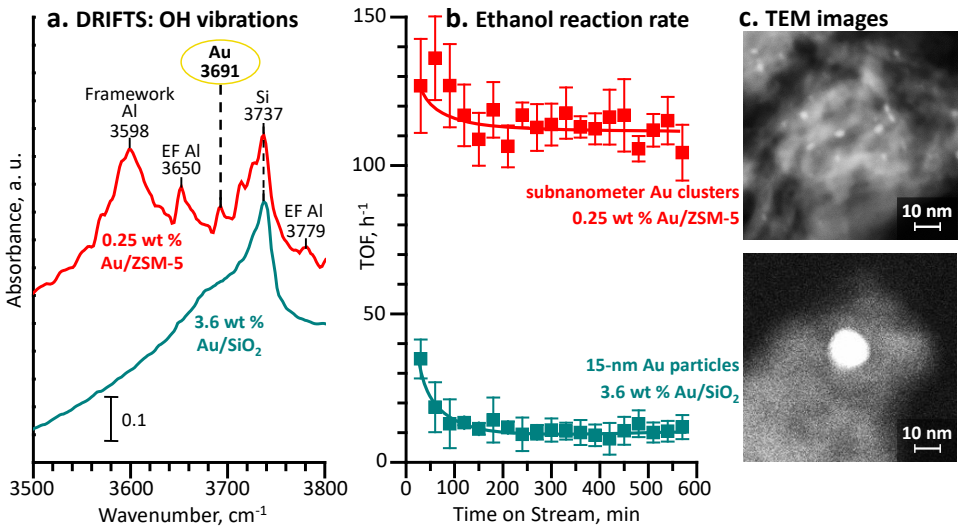

Figure 3. (**a**) DRIFTS spectra, (**b**) ethanol reaction rates in selective oxidation with gas-phase oxygen in a flow reactor at 333 K and atmospheric pressure and (**c**) TEM images for 0.25 wt % Au/ZSM-5 and 3.6 wt % Au/SiO_2. These catalysts had the same number of surface Au atoms.

of the Au surface and functional properties associated with the presence of coordinatively unsaturated surface Au atoms, such as catalytic activity. In catalytic selective oxidation of ethanol with gas-phase oxygen, the reaction activity of subnanometer Au particles, for which hydroxyls were observed, was 10 times higher than that of 15-nm Au particles, for which hydroxyls were not observed, when the total number of surface Au atoms for both catalysts was the same.

The findings that hydroxyls on Au can be directly observed spectroscopically, that their O-H stretching vibration is insensitive to the size of Au structures and that the presence of this vibration is a qualitative indicator of the surface functional properties, such as catalytic activity, will be useful in the development of more efficient Au-based catalysts for selective hydrocarbon oxidation in the transition to green chemistry and sustainability, in the development of improved sensors, medical diagnostics and in multiple other research and industrial applications.

Notes and references

There are no conflicts to declare. This research was supported by the U.S. Department of Energy, Office of Science, Office of Basic Energy Sciences, under Award DE-SC0019052. The DFT calculations were performed with the Materials Studio software provided by Dassault Systèmes BIOVIA Corporation under a collaborative research agreement. We thank Dr. Felix Hanke and Dr. Victor Milman at Dassault Systèmes BIOVIA Corporation for discussions on the computational settings. We thank Ari Gilman at Princeton University for help with the DRIFTS measurements.

1. Y.-Y. Kim, R. Darkins, A. Broad, A. N. Kulak, M. A. Holden, O. Nahi, S. P. Armes, C. C. Tang, R. F. Thompson, F. Marin, D. M. Duffy and F. C. Meldrum, *Nat. Commun.*, 2019, **10**, 5682.
2. Z. Chen and E. A. Rozhkova, *Nat. Nanotech.*, 2018, **13**, 880-881.
3. G. Ortega, M. Kurnik, B. K. Gautam and K. W. Plaxco, *J. Am. Chem. Soc.*, 2020, **142**, 15349-15354.
4. W. Sun, L. Luo, Y. Feng, Y. Cai, Y. Zhuang, R.-J. Xie, X. Chen and H. Chen, *Angew. Chem., Int. Ed.*, 2020, **59**, 9914-9921.
5. X.-P. Fu, L.-W. Guo, W.-W. Wang, C. Ma, C.-J. Jia, K. Wu, R. Si, L.-D. Sun and C.-H. Yan, *J. Am. Chem. Soc.*, 2019, **141**, 4613-4623.
6. M. S. Ide and R. J. Davis, *Acc. Chem. Res.*, 2014, **47**, 825-833.
7. K. Liu, T. Chen, S. He, J. P. Robbins, S. G. Podkolzin and F. Tian, *Angew. Chem.*, 2017, **129**, 13132–13137.
8. K. Liu, T. Chen, S. He, J. P. Robbins, S. G. Podkolzin and F. Tian, *Angew. Chem., Int. Ed.*, 2017, **56**, 12952-12957.
9. D. G. Barton and S. G. Podkolzin, *J. Phys. Chem. B*, 2005, **109**, 2262-2274.
10. Y. Zheng, Y. Tang, J. R. Gallagher, J. Gao, J. T. Miller, I. E. Wachs and S. G. Podkolzin, *J. Phys. Chem. C*, 2019, **123**, 22281-22292.
11. T. Chen, E. Kertalli, T. A. Nijhuis and S. G. Podkolzin, *J. Catal.*, 2016, **341**, 72-81.
12. J. Gao, Y. Zheng, Y. Tang, J. M. Jehng, R. Grybos, J. Handzlik, I. E. Wachs and S. G. Podkolzin, *ACS Catal.*, 2015, **5**, 3078-3092.
13. J. Gao, Y. Zheng, J. M. Jehng, Y. Tang, I. E. Wachs and S. G. Podkolzin, *Science*, 2015, **348**, 686-690.
14. J. Gao, Y. Zheng, G. B. Fitzgerald, J. de Joannis, Y. Tang, I. E. Wachs and S. G. Podkolzin, *J. Phys. Chem. C*, 2014, **118**, 4670-4679.
15. J. P. Robbins, L. Ezeonu, Z. Tang, X. Yang, B. E. Koel and S. G. Podkolzin, *ChemCatChem*, 2022, e202101546.
16. K.-I. Ataka and M. Osawa, *Langmuir*, 1998, **14**, 951-959.
17. H. Ibach, *Surf. Sci.*, 2010, **604**, 377-385.
18. S. G. Podkolzin, O. V. Manoilova and B. M. Weckhuysen, *J. Phys. Chem. B*, 2005, **109**, 11634-11642.
19. S. G. Podkolzin, E. E. Stangland, M. E. Jones, E. Peringer and J. A. Lercher, *J. Am. Chem. Soc.*, 2007, **129**, 2569-2576.
20. A. W. A. M. van der Heijden, S. G. Podkolzin, M. E. Jones, J. H. Bitter and B. M. Weckhuysen, *Angew. Chem., Int. Ed.*, 2008, **47**, 5002-5004.
21. J. Kim, J. Fu, S. G. Podkolzin and B. E. Koel, *J. Phys. Chem. C*, 2010, **114**, 17238-17247.
22. J. Kim, L. A. Welch, A. Olivas, S. G. Podkolzin and B. E. Koel, *Langmuir*, 2010, **26**, 16401-16411.
23. J. Gao, H. Zhao, X. Yang, B. E. Koel and S. G. Podkolzin, *ACS Catal.*, 2013, **3**, 1149-1153.
24. J. Gao, H. Zhao, X. Yang, B. E. Koel and S. G. Podkolzin, *Angew. Chem., Int. Ed.*, 2014, **53**, 3641-3644.
25. T. Chen, A. Pal, J. Gao, Y. Han, H. Chen, S. Sukhishvili, H. Du and S. G. Podkolzin, *J. Phys. Chem. C*, 2015, **119**, 24475–24488.
26. E. V. Scoullos, M. S. Hofman, Y. Zheng, D. V. Potapenko, Z. Tang, S. G. Podkolzin and B. E. Koel, *J. Phys. Chem. C*, 2018, **122**, 29180-29189.
27. M. S. Hofman, E. V. Scoullos, J. P. Robbins, L. Ezeonu, D. V. Potapenko, X. Yang, S. G. Podkolzin and B. E. Koel, *Langmuir*, 2020, **36**, 8705-8715.
28. Z. Tang, T. Chen, K. Liu, H. Du and S. G. Podkolzin, *Langmuir*, 2021, **37**, 11603–11610.
29. R. G. Greenler, D. R. Snider, D. Witt and R. S. Sorbello, *Surf. Sci.*, 1982, **118**, 415-428.
30. Y. Zheng, Z. Tang and S. G. Podkolzin, *Chem. Eur. J.*, 2020, **26**, 5174-5179.